Pertanika J. Sci. & Technol. 26 (2): 829 - 840 (2018)

SCIENCE & TECHNOLOGY

Journal homepage: http://www.pertanika.upm.edu.my/

A Mono-Window Algorithm for Land Surface Temperature Estimation from Landsat 8 Thermal Infrared Sensor Data: A Case Study of the Beas River Basin, India

Gopinadh Rongali*, Ashok Kumar Keshari, Ashvani Kumar Gosain and Rakesh Khosa

Department of Civil Engineering, Indian Institute of Technology Delhi, New Delhi, Delhi 110016, India

ABSTRACT

Land surface temperature (LST) is estimated using thermal infrared remote sensing data, which record the apparent temperature of the earth's surface by measuring the radiant energy of its surface. However, it is also possible to estimate LST through satellite images and image processing software. The Landsat 8 satellite was successfully launched in 2013, with two thermal infrared bands for continuous earth observations to provide for the estimation of LST. However, the calibration notifications issued by the United States Geological Survey (USGS) indicate that the data from the Landsat 8 thermal infrared sensor (TIRS) Band 11 show large uncertainty and thus, it was suggested to use TIRS Band 10 data as a single spectral band for LST estimation. In this study, we present a mono-window (MW) algorithm for LST estimation from the Landsat 8 (Path-147 and Row-38) using TIRS Band 10 data with a 100-m resolution. Emissivity was derived with the help of the normalised difference vegetation index (NDVI) proportion of vegetation technique for which operational land imager (OLI) Bands 4 and 5 (30-m resolution) were used. The results show that the LST was higher in the regions of barren land but lower in snow-covered areas. Further, the LST results were also compared with the air temperature data and they were found to be in good agreement. The MW algorithm presented in the study could be used as an efficient method for LST estimation from the Landsat 8 TIRS Band 10 data.

Keywords: Land surface temperature, landsat 8 TIRS, mono-window algorithm, NDVI, OLI

Article history:
Received: 12 December 2017
Accepted: 28 March 2018

E-mail addresses:
gopinadh01@gmail.com (Gopinadh Rongali)
akeshari@civil.iitd.ac.in (Ashok Kumar Keshari)
gosain@civil.iitd.ac.in (Ashvani Kumar Gosain)
rkhosa@civil.iitd.ac.in (Rakesh Khosa)
*Corresponding Author

ISSN: 0128-7680 © 2018 Universiti Putra Malaysia Press.

INTRODUCTION

Remote sensing is the acquisition of information about an object from the electromagnetic spectrum without making physical contact with an object. Nowadays, advanced satellite data has widely been used in environmental and climate change

studies. Thermal bands of Landsat 8 are significant data for land surface temperature (LST) calculation. LST has been identified as a significant variable of microclimate and radiation transfer within the atmosphere (Rajendran & Mani, 2015). Further, land use/land cover (LULC) of an area is also an important factor in the estimation of LST. Natural and anthropogenic activities change the physical and biological conditions of a region, and this in turn affects the LST of that area. With a change in LST value, the local climate of an area also changes (Rajeshwari & Mani, 2014). The traditional way of surface temperature estimation, such as through monitoring by a meteorological department weather station and other public and private sector observation methods, is not feasible for all types of terrain condition; in addition, they are also time consuming. However, remote sensing satellites can provide data for any topographic and climatic condition of a region, especially distinctive local climates (microclimates) produced by different land surfaces. The National Aeronautics and Space Administration (NASA) Landsat programme provides different spatial resolution satellite images for various time periods. Landsat 8 captures two different sets of images, one from OLI with nine bands (with 30-m resolution) and the second from TIRS with two bands (Band 10 and Band 11 with 100 m resolution) that are useful in providing more accurate surface temperatures. The TIRS uses quantum well infrared photo detectors (QWIPs) to detect the long wavelengths of light emitted from the earth surface whose intensity depends on surface temperature. As surface temperatures are directly related to surface physical properties, the normalised difference vegetation index (NDVI) analysis is an ideal approach for estimating LST in the Himalayan landscape.

LITERATURE REVIEW

Land surface integrated with temperature is identified as a significant variable to study the microclimate and radiation transfer within the atmosphere. As LST is the skin temperature of surface soil-water content and vegetation cover (Rajendran & Mani, 2015), it is very important to consider in climate change studies. Srivanit, Hokao and Phonekeo (2012) used Landsat thematic mapper (TM) imagery from 1994, 2000 and 2009 to identify the thermal characteristics of the rapidly urbanised Bangkok metropolitan area by investigating the correlation between the LST and NDVI. In their study, LST and NDVI were found to be closely correlated in several LULC categories, particularly in vegetated areas. Decrease of biomass primarily triggered the impacts of urban expansion on LST. Similarly, Li et al. (2004), and Giannini, Belfiore, Parente and Santamaria (2015) suggested the use of high resolution sequence satellite data for the analysis of LST over a watershed area in Lowa, Bangkok. LST images were extracted from the Landsat 5 TM and Landsat 7 enhanced thematic mapper (ETM) thermal bands. The NDVI was derived from visible and near-infrared bands (Band 4 and Band 5) of Landsat to estimate emissivity for Landsat thermal bands. The estimated LST values were compared with ground truth data measurements. The actual difference between the LST estimated from Landsat 5 and 7 and the ground truth actual measurements was 0.98^0C and 1.47^0C, respectively. Thus, the spatial differences of LST were identified using these satellite images. In another study, Dagliyar, Avdan, Yildiz and Nefeslioglu (2015) used Landsat TIRS and OLI data to estimate

the LST variation over Thiruvananthapuram, capital city of the state of Kerala, India. In their study, potentials of semi-automatic classification plug-in integrated with the open-source geographical information system package quantum (QGIS) were utilised for image acquisition, pre-processing, land cover classification and derivation of LST from land surface. LST of the urban Erzurum was estimated using Landsat 8 OLI and TIRS having 12-bit radiometric resolution and evaluated on the basis of surface emissivity and brightness values. In order to validate the LST derived from Landsat 8 bands, kinetic surface temperature measurements acquired from the general directorate of the state meteorological service in and around the study area were incorporated. The results showed that maximum temperature difference was around 6.45^0C, while the minimum difference was around 1.86^0C. In this study also, temperature difference was observed between LULC and LST derived from Landsat 8. Furthermore, the studies by Lv and Zhou (2011), Suresh, Ajay and Mani (2016) and Ning, Gao, Meng, Xu and Gao (2017) identified the relationship between LULC change and the LST using Landsat 5 TM and ETM images. In order to derive land use classification, the object-based method was used. The retrieval of LST was followed by the use of the MW algorithm. The derived results indicated that LST was highly influenced by the LULC. Similarly, LST was also found to be positively correlated with impervious surface and vice versa. These studies strongly recommended that such a study should be applied in regions with a trend of rapid urbanisation. Recently, Landsat 5 TM and Landsat ETM for the years 1990, 2001 and 2010 were used to estimate LST using the Landsat 7 user handbook method in Devikulam *taluk*. The results showed that the mean temperature was increasing steadily (Suresh et al., 2016).

The literature concluded that land surface temperature (LST) is an important factor and it needs to be considered in climate change studies. Further, the estimation of the accuracy of the LST using advanced satellite data (i.e. Landsat 8) is very important as it affects accuracy directly. However, so far very few studies have used the advanced TIRS data. In this research, we used TIRS data from the Landsat 8 satellite to study the Beas river basin area to estimate LST.

The Study Area

The Beas river basin is located in the state of Himachal Pradesh, India (Figure 1). The study area is between 31°N and 32°N (latitude) and 77°E and 78°E (longitude) and covers an area of 5383 km^2, with elevation ranging from 857 m to 6582 m. The catchment area mostly contains impulsive slopes and the rocks are commonly bare. In winter, most of the river is snow and later in summer, the Beas river basin is mostly fed by snowmelt. The Beas river basin gets heavy rainfall during the monsoon season, with rain normally falling from July to late September. It collects the moisture comportment of the winds from both the Arabian Sea and the Bay of Bengal. The upper portion of the basin receives snowfall during winter.

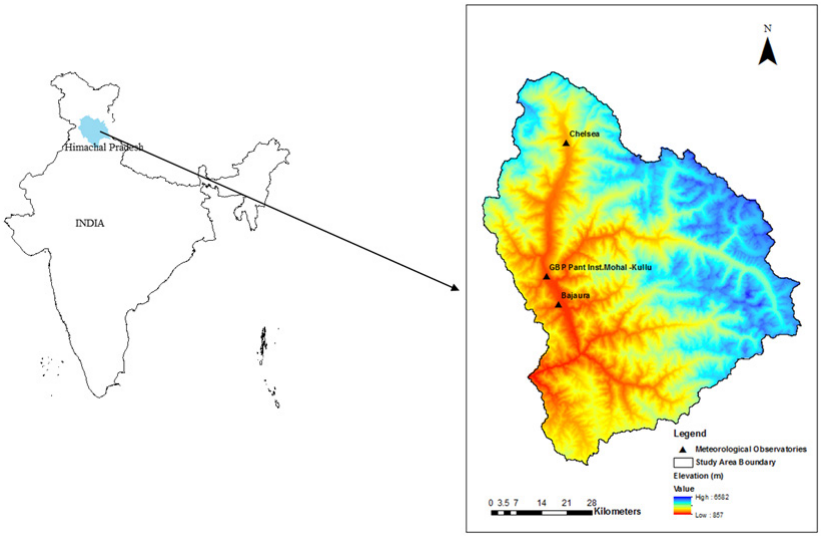


Figure 1. The Beas river basin up to Pandoh dam showing the available climate stations

METHODS AND DATA USED

In this study, Landsat 8 OLI and the TIRS image of 24 April, 2015 (Path/Row - 147/38) pertaining to the study area was used to calculate NDVI and LST. A digital elevation model (DEM) of the study area at 30 m spatial resolution, extracted from the advanced space borne thermal emission and reflection radiometer (ASTER) giving global DEM for the Beas river basin was downloaded from the USGS earth explorer data centre website (https://earthexplorer.usgs.gov/). Further, air temperature data were downloaded from the National Remote Sensing Centre's (NRSC) Meteorological and Oceanographic Satellite Data Archival Centre (MOSDAC) website (http://www.mosdac.gov.in/) for three ground stations (Chelsea, GB Pant Inst. Mohal-Kullu and Bajaura) located within the Beas river basin (Figure 1). Later, the MW algorithm method was employed to calculate the LST in the study area. Vegetation proportion calculation, emissivity calculation, LST calculation etc. were executed using the ArcGIS 10.3 software platform. A detailed description of the methodology is outlined in Figure 2.

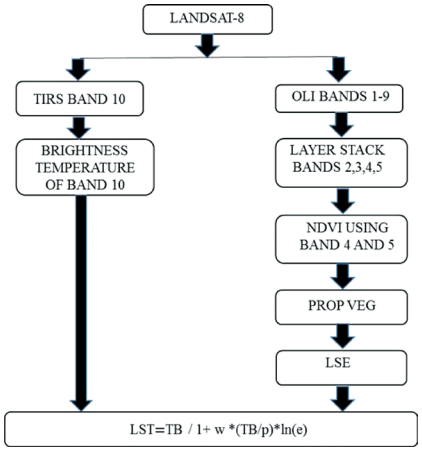


Figure 2. Flow chart of the Mono-Window algorithm

Image Acquisition and Pre-Processing

The images were already rectified to WGS-1984-UTM-Zone_43N. In the next step, the conversion of digital number (DN) to the physical measure of top of atmospheric (TOA) reflectance given in the metadata file and the thermal band at satellite brightness temperature (TB) was done. Later, the file with extension of ".MTL" was provided in the Landsat 8 image set, which contains the thermal constants needed to convert TIRS data using the satellite TB. Lastly, TIRS band data were used to convert spectral radiance to TB by processing thermal constants provided in the metadata file (Table 1 to 3).

Table 1
Landsat 8 metadata of the Beas river basin

Sensor	No. of Bands	Resolution (m)	Path/Row	Date of Acquisition
OLI	9	30	147/38	24 April, 2015
TIRS	2	100		

Table 2
K1 and K2 values

Thermal Constant	Band 10
K1	1321.08
K2	777.89

Table 3
Rescaling factor

Rescaling Factor	Band 10
M_L	0.0003342
A_L	0.1

RESULTS AND DISCUSSION

LST Calculation Using Mono-Window Algorithm for Landsat 8 Data

The primary objective of the study was to estimate land surface temperature (LST) as well as vegetation index using Landsat 8 data. The LST and NDVI obtained were for the year 2015. The Landsat 8 TIRS sensors acquired temperature data and stored this information as a digital number (DN) ranging between 0 and 255. Generally, the LST can be estimated by applying structured mathematical algorithms such as mono-window (MW), split-window (SW), single channel (SC) and multi angle (MA) algorithm. These algorithms use the TB of the TIRS band, mean and difference in land surface emissivity for estimating the LST of an area. In the present study, the MW algorithm has been used to estimate the LST. The detailed step-by-step procedure for LST calculation is given below.

$$LST = TB/1 + W * (TB/p) * \ln(e) \quad (1)$$

where,

LST = Land surface temperature (K)

TB = At satellite temperature (K)

W = Wavelength of emitted radiance $(11.5 \mu m)$

$p = h * c/s (1.438 * 10^{-2} mK)$

h =Planck's constant $(6.626 * 10^{-34} Js)$

s = Boltzmann constant $(1.38 * 10^{-23} J/K)$

c = Velocity of light $(2.998 * 10^{8} m/s)$

p =14380

Step 1. We converted the DN to radiance using the given formula, where $L\lambda$ is the spectral radiance at the sensor aperture $(watts/(m^2 * ster * \mu m))$

$$L\lambda = M_L Q_{cal} + A_L \quad (2)$$

where,

$L\lambda$ = TOA spectral radiance $(watts/(m^2 * ster * \mu m))$

M_L = Band specific multiplicative rescaling factor from the metadata (Radiance_mult_Band_X, where X is the band number 10)

A_L = Band specific additive rescaling factor from the metadata (Radiance_add_Band_X, where X is the band number 10)

Q_{cal} = Quantised and calibrated standard product pixel value (DN)

Here, $L\lambda$ for the study area was $L\lambda$ = 0.0003342 * Band 10 + 0.1, resulting in the value of radiance Band 10.

Step 2. We converted the band radiance (which was derived from Equation 2) to TB using the thermal constant given in metadata file (Table 2). The conversion formula is given below:

$$T = K2/l_n(K1/L\lambda + 1) - 273.15 \quad (3)$$

where,

T = At satellite brightness temperature in Kelvin (K)

$L\lambda$ = TOA spectral radiance $(watts/(m^2 * ster * \mu m))$

$K1$ = Band_specific thermal conversion from the metadata

($K1$ – Constant_Band_X, where X is the band number, 10)

$K2$ = Band_specific thermal conversion from the metadata

($K2$ – Constant_Band_X, where X is the Band number, 10)

273.15 = Convert Kelvin to ^{o}Celsius

According to Equation 3, T can be calculated for the study area as $T = 1321.08 / l_n(774.89 / Band10radiance + 1) - 273.15$. From the formula, we can get Band 10 sattemp as an output. It shows the TB in °Celsius.

Step 3. We found the temperature of Band 10 sattemp using the cell statistics tool and we got the Band 10 sattemp as an output. Here, the minimum temperature was -14.6673^{0}C, while the maximum temperature was 33.0782^{0}C.

Step 4. We estimated land surface emissivity (LSE) using the given equation.

$$e = 0.004P_V + 0.986 \tag{4}$$

e = Emissivity
P_V = Proportion of vegetation that is calculated using the NDVI value
$NDVI$ = Normalised difference vegetation index
NDVI can be calculated in ArcGIS by applying the given formula

$$Float(Band5 - Band4) / Float(Band5 + Band4) \tag{5}$$

where,
$Band5$ = Near infrared (NIR - 0.85–0.88 μm) Band, $Band4$ = Red Band (0.64–0.67 μm) wavelengths from the $NDVI$ result, The $NDVI_{\min}$ value was – 0.453896 and the $NDVI_{\max}$ value was 0.81123 (Figure 3). We substituted these values in Equation 6 and derived the proportion of vegetation (P_V).

$$P_V = (NDVI - NDVI_{\min} / NDVI_{\max} - NDVI_{\min})^2 \tag{6}$$

In ArcGIS, this can be done by applying this formula:
Square $(NDVI + 0.453896 / 0.81123 + 0.453896)$.

From this we derived the $PROPVEG$ as an output of the proportion of vegetation. Then we calculated LSE by applying the P_V value in Equation 4: $0.004 * PROPVEG + 0.986$. From this we got the LSE of the study area, which is shown in Figure 4.

Step 5. We estimated LST using Equation 1. The output such as Band 10 sattemp was substituted for BT that was in ^{0}C, and the LSE value was replaced by 'e', that is, emissivity. Equation 1 is: $LST = BT / 1 + W * (BT / p) * l_n(e)$. In ArcGIS it can be done using this formula:

$$LST = "Band10sattemp" / 1 + "Band10" * ("Band10sattemp" / 14380) * l_n("LSE")$$

Finally, we got the actual LST of Band 10 of the study area (Figure 5). Table 4 gives the statistics of the study area's LST. Sun elevation of 62.54660086 represents the Landsat 8 image acquisition time that was probably in the morning.

Figure 5 shows the spatial distribution of the estimated LST for the year 2015. The maximum and minimum temperature and statistics of the LST are shown in Table 4, -14.667°C and 33.078°C, respectively, with a mean average of 9.546°C. The archive meteorological

observatory data obtained from the MOSDAC was compared with the estimated LST. The satellite derived estimates for the LST and MOSDAC climate station observed temperature were comparable and validated the findings of the estimated temperature. The MOSDAC observations and satellite-derived LST were nearly in agreement with respect to temperature values in the respective year. The LST output portrayed that it varied from -14.667ºC to 33.078ºC. The highest LST values were traced in the southern plains of the study area. However, the lowest LST values were seen in the highly elevated regions that experienced snow fall.

The NDVI map (Figure 3) represents the Beas river basin on 24 April, 2015 derived from Band 5 (NIR) and Band 4 (RED) of the OLI sensor using the ArcGIS 10.3 raster calculator. The range of NDVI varied from -0.453 to 0.8112 for MW algorithm (zero for negative NDVI values using conditions). The southwestern part of the Beas river basin had the highest NDVI value, whereas the area under snow fall had a negative value (Figure 3). The value of the NDVI was later used to calculate the proportion of vegetation using Equation 6 and the LSE was calculated using Equation 4. Later, we implemented equations in the ArcGIS 10.3 raster calculator to calculate the LSE map shown in Figure 4 from the MW algorithm. The LSE of the Beas river basin ranged between 0.987 and 0.999. Highly elevated regions in the basin had more snow cover; hence, LSE was low in these regions. High LSE was found in the western and southwestern parts of the basin, whereas low LSE was noticed in the northern and eastern parts of the study area. Further, the TIRS Band 10 was used to estimate the TB in Celsius using the algorithm described in Equation 3. Similarly, equation 1 was used to estimate the LST using the raster calculator. Figure 5 represents the final LST image of the Beas river basin seen on 24 April, 2015.

LST Validation

The two major LST validation models were obtained through ground measurements or near-surface air temperature (Srivastava, Majumdar, & Bhattacharya, 2009; Li et al., 2013). The LST results comparing with the ground measurements results may have an error of up to 5°C; in the case of Srivastava et al. (2009), the accuracy of the results in some areas showed a difference of ±2°C with actual ground temperature measurements. According to Li et al. (2013), another method using the mean near-surface air temperature to verify the retrieved LST results showed that the LST retrieving error was about 0.7°C.

As such, no ground measurements of LST were available on the field; the LST obtained from Landsat 8 were compared with the air temperature observed at three stations. The comparison was made for air temperature, which is different and can sometimes result in big differences since the resolution of Landsat 8 for the used bands is 100 m for the thermal band and 30 m for the red and NIR bands. The LST was calculated and taken according to the pixel used by the respective meteorological stations. The relationship between air temperature and LST seen from Landsat 8 data, depicted in Figure 6, is in close agreement. In general, air temperature was higher than LST.

Sometimes, the differences can be great depending on weather conditions and other factors (Gallo, Hale, Tarpley, & Yu, 2011). It should also be taken into consideration that there is a 1.1-to-2-m difference between the LST and the air temperature, which means that differences in the temperatures are normal and expected.

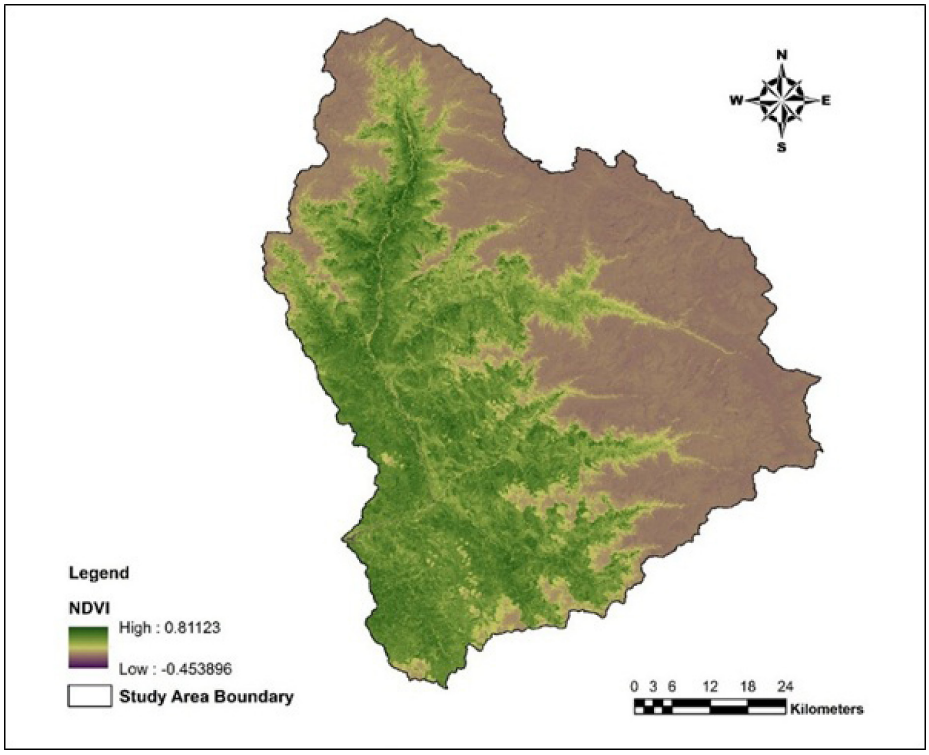


Figure 3. NDVI map of 24 April, 2015 from Mono-Window algorithm

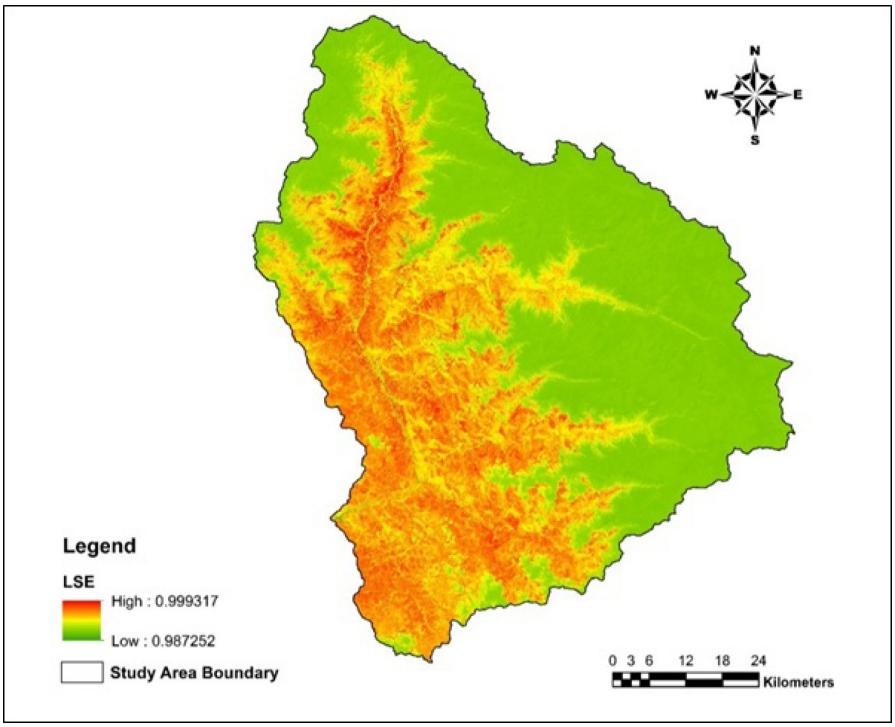


Figure 4. LSE map of 24 April, 2015 from Mono-Window algorithm

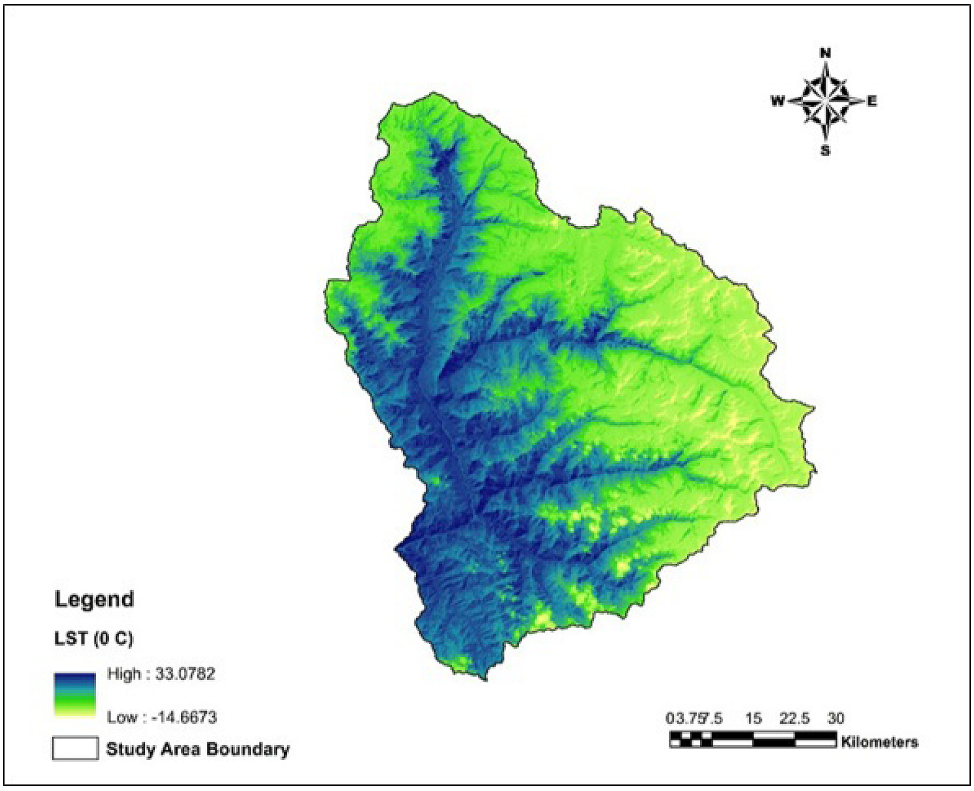


Figure 5. LST map of 24 April, 2015 from Mono-Window algorithm

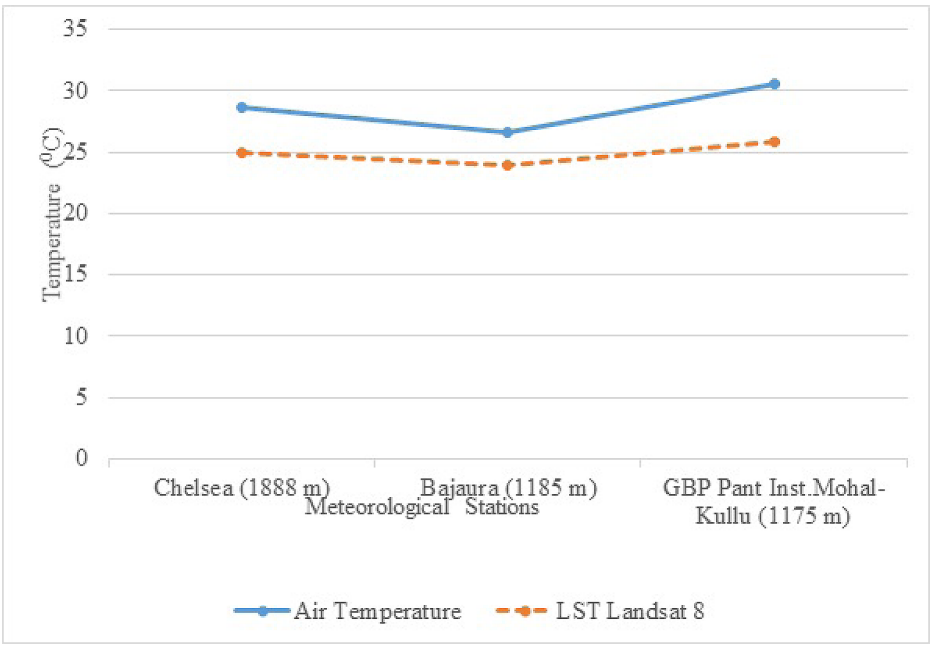


Figure 6. Comparison between air temperature data and LST values from Landsat 8 on 24 April, 2015 at three different stations

Table 4
Statistics of landsat 8 lst of Beas river basin

Statistics of Landsat 8 LST	
Sensor	TIRS
Minimum temperature	-14.667
Maximum temperature	33.078
Mean temperature	9.546
Standard deviation	10.073

CONCLUSION

In this paper, the potential of remote sensing to study temperature variation in the Beas river basin by estimating LST distribution with the help of the Landsat 8 OLI and TIRS sensor was studied. The MW algorithm method was applied to estimate the LST from the TIRS data. The analysis of the results suggested that the heat energy radiated by the earth's surface determined factors such as different types of land use, vegetation cover, soil and snow in the study area, revealing the variation in surface temperature for different surface patterns. It was also evident from the results that surface temperature variation controlled surface heat and water exchange with the atmosphere, resulting in climate change in the region. Some climatic phenomena play a minor role in temperature variation, but some play a major role. Activities such as land conversion due to rapid tourism development, ever increasing automobile carbon emission, firewood combustion from kitchens, periodical removal of firewood, for example eucalyptus, and forests replaced by settlement and restaurants etc. result in higher temperature variation. Remote sensing technology data such as Landsat 8 TIRS provides an efficient way to estimate LST. The results documented in this study can help in estimating weather phenomena such as microclimate, heat pockets and maximum temperature in vulnerable regions in the study area and also help in deciding what necessary scientific actions can be taken like reforestation, frequent checking of vehicles for pollution and reduced plastic incineration to curb temperature increase.

ACKNOWLEDGEMENT

The authors highly appreciate the USGS earth explorer for providing the Landsat 8 and ASTER GDEM data. We also thank the NRSC, Hyderabad, India for providing the air temperature data downloaded from the MOSDAC website that were used in this study.

REFERENCES

Dagliyar, A., Avdan, U., Yildiz, N. D., & Nefeslioglu, H. A. (2015). Determination of land surface temperature using Landsat 8 TIRS: A case study in Erzurum, Turkey. *Geophysical Research Abstracts, 17,* EGU2015-11007.

Gallo, K., Hale, R., Tarpley, D., & Yu, Y. (2011). Evaluation of the relationship between air and land surface temperature under clear- and cloudy-sky conditions. *Journal of Applied Meteorology and Climatology, 50*(3)*,* 767–775.

Giannini, M. B., Belfiore, O. R., Parente, C., & Santamaria, R. (2015). Land surface temperature from Landsat 5 TM images: Comparison of different methods using airborne thermal data. *Journal of Engineering Science and Technology Review, 8*(3)*,* 83–90.

Li, F., Jackson, T. J., Kustas, W. P., Schmugge, T., French, A., Cosh, A. M., & Bindlish, R. (2004). Deriving land surface temperature from Landsat 5 and 7 during SMEX02/SMACEX. *Remote Sensing of Environment, 92*(4)*,* 521–534.

Li, Z. L., Tang, B. H., Wu, H., Ren, H., Yan, G., Wan, Z., … & Sobrina, A. J. (2013). Satellite-derived land surface temperature: Current status and perspectives. *Remote Sensing of Environment, 131,* 14–37.

Lv, Z., & Zhou, Q. (2011). Utility of Landsat image in the study of land cover and land surface temperature change. *Procedia Environment Science, 10,* 1287–1292.

Ning, J., Gao, Z., Meng, R., Xu, F., & Gao, M. (2017). Analysis of relationships between land surface temperature and land use changes in the Yellow River delta. *Frontiers of Earth Science,* 1–13.

Rajendran, P., & Mani, K. (2015). Estimation of spatial variability of land surface temperature using Landsat 8 imagery. *International Journal of Engineering and Science, 11*(4), 19–23.

Rajeshwari, A., & Mani, N. D. (2014). Estimation of land surface temperature of dindigul district using Landsat 8 data. *International Journal of Research in Engineering and Technology, 3*(5), 122–126.

Srivanit, M., Hokao, K., & Phonekeo, V. (2012). Assessing the impact of urbanization on urban thermal environment: A case study of Bangkok metropolitan. *International Journal of Applied Science and Technology, 2*(7)*,* 243–254.

Srivastava, P., Majumdar, T. J., & Bhattacharya, A. K. (2009). Surface temperature estimation in Singhbhum shear zone of India using Landsat-7 ETM+ thermal infrared data. *Advances in Space Research, 43*(10), 1563–1574.

Suresh, S., Ajay, S. V., & Mani, K. (2016). Mountain landscape of Devikulam Taluk using Landsat 8 Data. *International Journal of Research in Engineering and Technology, 5,* 92–96.